ScienceDirect

Improving reference evapotranspiration (ET_o) calculation under limited data conditions in the high Tropical Andes

Cristina Vásquez [a, b] 👤 ✉, Rolando Célleri [a, b], Mario Córdova [a], Galo Carrillo-Rojas [a, c]

Show more ⌄

☰ Outline ｜ ⤳ Share 💬 Cite

Get rights and content

Highlights

- Methods to estimate R_s and VPD based on T were evaluated for the Andean Páramo.

- Assuming T_{min} for dewpoint T to estimate the actual vapor pressure was successful.

- The error (%) in daily ET_o estimations was lower than the error found for daily R_s estimations.

- The estimation of ET_o using the most accurate methods to replace measurements was satisfactory.

Abstract

The computation of the reference crop <u>evapotranspiration</u> (ET_o) using the FAO56 Penman-Monteith equation (PM-ET_o) requires data on maximum and minimum air temperatures

(T_{max}, T_{min}), relative humidity (RH), solar radiation (R_s), and wind speed (u_2). However, the records of meteorological variables are often incomplete or of poor quality. Frequently, in the mountain areas such as those of the Andes, environmental sensors are subject to harsh conditions, due to the diurnal/nocturnal climatic variability causing challenging conditions for meteorological monitoring, which leads to data loss. For high-elevation landscapes like the Andes, the missing variables of vapor pressure deficit and solar radiation cause a high impact on PM-ET_o calculation. To assess these limitations, several methods relying on maximum and minimum temperature to estimate the missing variables have been considered in the present investigation. Based on data from three automatic weather stations in the high Tropical Andes (humid páramo, 3298 – 3955 m a.s.l.), we found that the calibration and validation of methods were essential to estimate R_s. Using the (De Jong and Stewart, 1993) (R_s-DS) method we retrieved the highest performance, a RMSE between 2.89 and 3.81 MJ m^{-2} day^{-1}. Moreover, In the absence of RH observations, replacing the dew point temperature (T_{dew}) by T_{min} was a reliable alternative, when apply the method of (Allen et al., 1998) (VPD-FAO) which showed the highest performance with RMSE between 0.08 and 0.12 kPa. These results yielded highly accurate PM-ET_o estimates, with RMSE between 0.29 and 0.34 mm day^{-1} and RMSE between 0.12 and 0.18 mm day^{-1}, respectively. As expected, when both variables were missing, the ET_o calculation increased its error, with an RMSE between 0.32 and 0.42 mm day^{-1}. A proper estimation of ET_o in the Andean páramo contributes to improved water productivity for domestic and industrial uses, irrigated agriculture, and hydropower.

<   Previous   Next   >

Keywords

Páramo; PM-ET_o; Solar radiation; Vapor pressure deficit; Calibration

1. Introduction

The páramo is the most important ecosystem in the high Tropical Andes for water resources supply (Hofstede et al., 2014). The Andean páramo covers over 30,000 km^2 of northern South America (Wright et al., 2018). It is the primary water source for communities located near this ecosystem, which include major cities in Colombia, Ecuador, and Perú (Buytaert et al., 2006). Its vegetation consists mainly of tussock grasses, cushion plants, and patches of woody species such as *Polylepis* sp. and *Gynoxys* sp. that occur only in sheltered locations and along water streams (Buytaert et al., 2006). This ecosystem serves as a sponge that captures precipitation, stores, and releases the water gradually to the surrounding areas (Llambí et al., 2012) producing a sustained streamflow during the year. This water resource is intensively used for irrigated agriculture, industry, rural, and urban drinking water systems, hydro-power production, and for sustaining aquatic ecosystems (Célleri and Feyen, 2009, Llambí et al., 2012). Particularly an important economic function of water in Andean ecosystems is to

irrigate agriculture in downstream areas. At present, irrigation represents 71.2%, which becomes the activity that consumes the most flow in our country. Compromising almost all of the water sources located in high altitude areas for irrigation (Ministerio de Agricultura y Ganadería et al., 2019).

Although evapotranspiration may not be a limiting factor for water use in cold and humid regions, the increasing demand for water resources due to population growth, urbanization, and irrigated agriculture require a reliable estimate of evapotranspiration to improve the yield and water productivity. A common approach for calculating evapotranspiration is the estimation of ET_o, which is the most useful for countless scientific and management applications, such as water balance studies at different scales, evaluation of water resources, and development of watershed management plans. Likewise, ET_o plays a key role in crop water, irrigation planning and management, as well as in studies related to the analysis of climate change and water conservation (Paredes et al., 2020, Paredes et al., 2017, Todorovic et al., 2013).

According to the Food and Agriculture Organization (FAO56) (Allen et al., 1998), the Penman-Monteith equation (PM) is the most recommended method to determine ET_o. This method is a global standard based on meteorological data (Allen et al., 1998) and their applications all over the world have been quite successful (Jabloun and Sahli, 2008, Ochoa-Sánchez et al., 2019, Paredes et al., 2020, Paredes et al., 2017, Paredes and Pereira, 2019, Todorovic et al., 2013). The major limitation of the Penman-Monteith equation reported in many studies is the requirement of meteorological variables (air temperature, relative humidity, solar radiation, and wind speed) that are often incomplete or of poor quality (Córdova et al., 2015, da Silva et al., 2018, Karimi et al., 2020, Paredes and Pereira, 2019, Santos et al., 2020, Sentelhas et al., 2010, Tomas-Burguera et al., 2017). This usually happens when a sensor breaks or malfunctions (e.g., due to weather conditions, lack of maintenance, or electronic failure). Frequently, in the mountain areas, like the Andes, sensors are subject to harsh environmental conditions, due to the high climatic variability during the day causing challenging environmental conditions for meteorological monitoring, which leads to data loss. Accordingly, the application of PM faces the problem of data unavailability.

Research has developed a variety of tools and procedures to overcome the unavailability of data by using empirical equations, most of them relying on maximum and minimum temperature. For instance, the procedures by Hargreaves and Samani (1982), the equations proposed in FAO56 (Allen et al., 1998), the equations by Castellví et al. (1997), among others. However, these methods require local calibrations to obtain satisfactory performances as several studies have shown in various climate types ranging from hyper arid to humid (Karimi et al., 2020, Paredes et al., 2017, Raziei and Pereira, 2013, Ren et al., 2016, Todorovic et al., 2013). The approach of these studies was the calibration of the K_{RS} coefficient of the Hargreaves and Samani (1982) method to estimate solar radiation when the variable was missing, and a correction in the minimum temperature to estimate actual vapor pressure in the absence of relative humidity data. In all cases, their results showed that the PM-ET_o method had greater precision in both arid and humid climates when missing data was estimated. However,

Todorovic et al. (2013) found that for good ET_o performance, the correction applied in the minimum temperature was only necessary for hyper-arid, arid, semi-arid, and dry subhumid climates and not for humid conditions. Moreover, Ren et al. (2016) found that the calibrated coefficient of the method to estimate solar radiation varied with climatic aridity. The errors of estimates were higher when the range of variation of ET_o was higher, which occurred more often for hyper-arid and arid climates contrarily to sub-humid locations. In addition, Karimi et al. (2020) also found that the effect of using estimated values of solar radiation on PM-ET_o calculation caused greater error than using estimated values of wind speed.

Unlike the most common methods reviewed above, in various studies, a large number of empirical methods are compared to estimate the missing variables (Bandyopadhyay et al., 2008, Besharat et al., 2013, Jabloun and Sahli, 2008, Li et al., 2013, Tabari et al., 2016). However, there is a shortage of information for high-elevation landscapes like the Andes, contrary to the information available in low and arid areas. Using daily data recorded from eight weather stations in North Africa (Tunisia), Jabloun and Sahli (2008) evaluated the performance of the PM-ET_o method with limited data and revealed that estimating solar radiation with Allen (1995) method that takes into account the elevation effects on the volumetric heat capacity of the atmosphere, it gave accurate estimates of ET_o in all the studied regions. Furthermore, the use of minimum temperature was a good alternative when relative humidity measurements were lacking. The use of the mean annual wind speed of the location led to acceptable ET_o estimates, especially for high ET_o rates. Under cool, arid, and semi-arid conditions in Iran, Tabari et al. (2016) estimated solar radiation using 12 models and then compared daily PM-ET_o values derived from both measured and estimated solar radiation. The results indicated that using estimated R_s, the PM-ET_o method performed well for semi-arid and arid climates. In cold conditions, the PM-ET_o accuracy decreased despite the calibration of the models.

There are also others alternatives to estimate meteorological variables, such us using satellite, geostatistical interpolation or machine learning. A complete review of this applications for ET_o estimation is beyond the scope of this paper, thus some relevant studies will be reviewed here. Silva et al. (2010) evaluated the use of mesoscale model results as proxy for weather variables in places where there are no meteorological stations and found that is the most effective method to generate estimates of ET_o. Feng et al. (2019) in temperate continental regions of China compared different machine learning and empirical models for global solar radiation prediction only using air temperature as inputs. The results indicated the hybrid mind evolutionary algorithm and artificial neural network model provided better estimations, compared with the existing machine learning and empirical models. Qadeer et al. (2021) applied the random forest (RF) approach to estimate the relative humidity as a function of dry- and wet-bulb temperatures. The RF model has sufficient potential to estimate RH. However, the prediction performance of the RF model strongly depends on both the quantity and quality of the training data. Berndt and Haberlandt (2018) investigated the performance of different interpolation techniques for various climate variables observed by weather stations in Northern Germany. They found that the influences of temporal resolution and spatial variability appear to be higher than the influence of station density. The best estimation accuracy is achieved for relative humidity and temperature due to the consideration of the

DEM and the low spatial variability. Jeong et al. (2017) compared geostatistical interpolation and stochastic simulation approaches for the estimation of daily solar radiation located across southern Canada. The three geostatistical interpolation models yield better performances at stations located in a high-density area of solar radiation measuring stations compared to the three stochastic simulation models. There is only one previous study that examined the impact of missing meteorological variables on PM-ET$_o$ calculation in the high Tropical Andes. Córdova et al. (2015) evaluated the PM-ET$_o$ equation with limited data using meteorological variables of two weather stations in the high Tropical Andes (Ecuador) and found that the maximum error in ET$_o$ calculations was observed when solar radiation and relative humidity were missing, while wind speed had a much lower impact. Finally, they concluded that there is an urgent need for the development of alternative methods in these sites to estimate accurate values for missing variables. There is a knowledge gap to estimate the missing variables and this makes PM-ET$_o$ subject to high uncertainty. Thus, the first step to achieving this is to develop or calibrate equations to estimate the missing variables and then evaluate its impact on PM-ET$_o$.

Therefore, the main goal of this article is to accurately estimate ET$_o$ when weather variables are lacking using PM method. The specific objectives of this study are (a) To calibrate and validate methods to estimate Rs from temperature data and to determine the method with the highest performance, (b) To evaluate the performance of methods to estimate Vapor Pressure Deficit (VPD) from temperature data and to determine the method with the highest efficiency and, (c) To evaluate the impact on PM-ET$_o$ calculation when R$_s$ and/or VPD are missing and these variables are estimated with the methods found in a) and b) in a páramo ecosystem.

2. Study area and data

In the Tropical Andes of southern Ecuador, the headwater catchment of Quinoas covers an area of about 94.1 km^2 and an elevation range of 3150–4425 m a.s.l. (Fig. 1). The Quinoas catchment is characterized as a Páramo ecosystem. This bioma stores large amounts of water that is captured from rainfall events, drizzle, and fog interception (Beck et al., 2008). The climate is influenced by air masses of both the Pacific and the Amazon basin (Buytaert et al., 2006). A bimodal precipitation seasonality is presented, in connection with the meridional displacement of the Intertropical Convergence Zone (ITCZ) and its double passage throughout the year over the deep tropics (Garreaud, 2009). This corresponds to the months from March to May and October where the maximum values of precipitation are recorded (Carrillo-Rojas et al., 2016). Annual precipitation is between 946 and 1120 mm. Table 1 shows the daily values of different meteorological variables. These values coincide with those reported by Córdova et al. (2015) and Carrillo-Rojas et al. (2016) in the same study site. Meteorological data were collected along an altitudinal gradient (3298–3955 m a.s.l.) during the six-year period 2014–2019 from three automatic weather stations (AWSs): Chirimachay, Virgen del Cajas (hereafter denoted as Virgen) and Toreadora. The climate is classified as Cfc according to the Köppen-Geiger categories Kottek et al. (2006), warm temperate climate, fully humid, with cool summer and cold winter in the three sites. Humid conditions were identified for the study area according to the aridity index. The aridity index was calculated

using the methodology of Padilla et al. (2011) which resulted from the ratios obtained by dividing rainfall by potential evapotranspiration. These indices were subsequently reclassified using the aridity classes proposed by UNEP (1992); the values were 1.6, 1.3, 1.5 for Chirimachay, Virgen and Toreador, respectively.
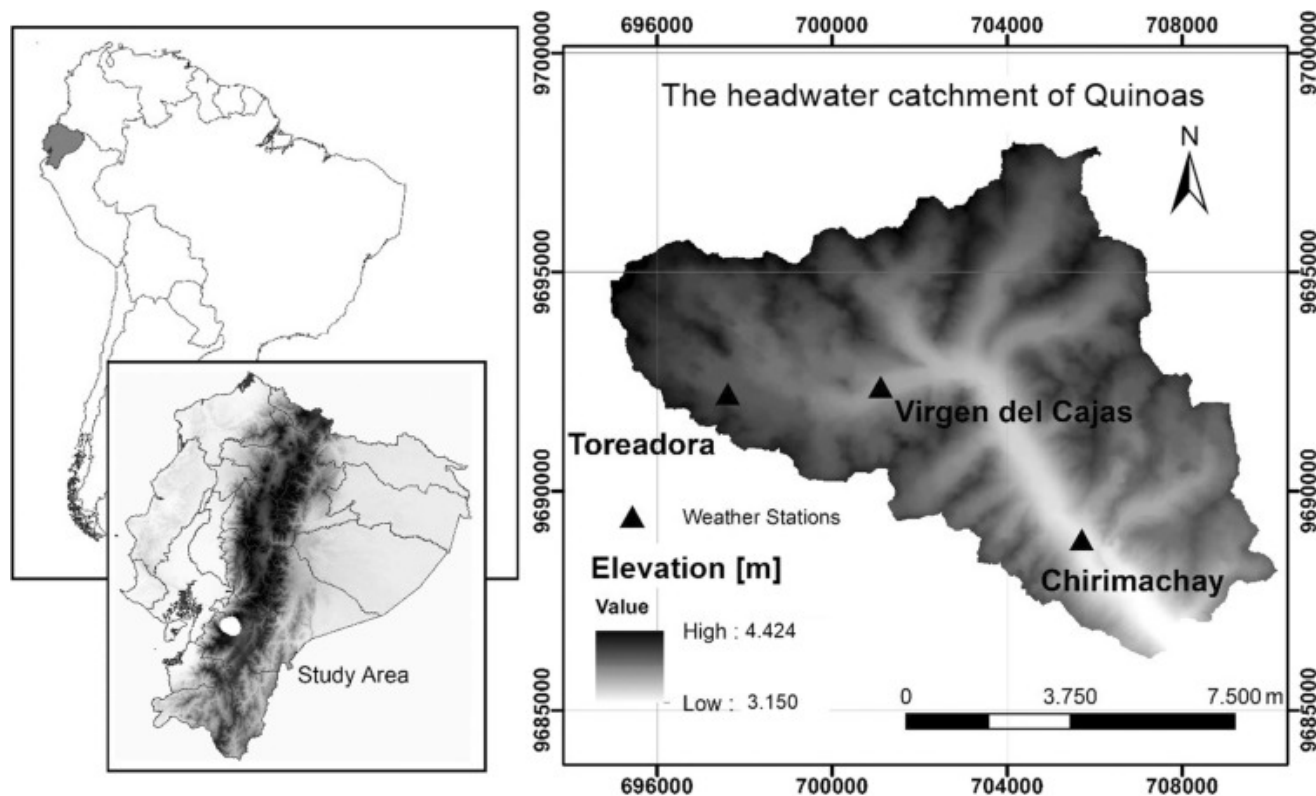
Download : Download high-res image (401KB)   Download : Download full-size image

Fig. 1. Study area and the location of weather stations in the Quinoas Ecohydrological Observatory.

Table 1. Summary of average values of daily meteorological variables during the study period 2014 – 2019. (Tmax, Tmin, HRmax, HRmin are absolute values).

Station name	Latitude and Longitude (UTM)	Elev. (m a.s.l.)	T_{avg} (°C)	T_{max} (°C)	T_{min} (°C)	RH_{avg} (%)	RH_{max} (%)	RH_{min} (%)	R_s (MJ m^{-2} day^{-1})	$U_{2\,m}$ (m s^{-1})	PM-ET$_o$ (mm day^{-1})	N' ob (d
Chirimachay	9688896;– 705704	3298	8.73	19.48	-1.35	85.26	100	8.81	10.12	1.38	1.88	21
Virgen	9623820;– 701111	3626	6.68	17.94	-3.92	83.01	100	9.52	11.56	1.58	1.98	21

Station name	Latitude and Longitude (UTM)	Elev. (m a.s.l.)	T_{avg} (°C)	T_{max} (°C)	T_{min} (°C)	RH_{avg} (%)	RH_{max} (%)	RH_{min} (%)	R_s (MJ m^{-2} day^{-1})	U_{2m} (m s^{-1})	PM-ET_o (mm day^{-1})	N° ob (d
Toreadora	9692227;– 697619	3955	5.46	17.15	-2.44	83.98	100	6.30	11.88	2.18	1.92	20

N° obs: number of observations.

The sites approached a reference ET_o station: an extensive surface of green, well-watered grass of uniform height, actively growing and shading the ground. All measurements were made at 2 m above ground level. Each station recorded data at a 5-minute frequency for average temperature (T_{avg}), T_{max}, T_{min}, average relative humidity (RH_{avg}), maximum relative humidity (HR_{max}), minimum relative humidity (HR_{min}), u_2 and R_s. The values were aggregated on a daily scale. Due to the presence of gaps in the database, preprocessing was performed, excluding days with missing data. The amount of missing data was 3.7%, 2.5%, and 6.8% for Chirimachay, Virgen, and Toreadora AWSs, respectively. In addition, data integrity was evaluated using guidelines suggested by Allen et al. (1998). These criteria included comparing measured solar radiation to theoretical solar radiation during clear-sky periods and comparing daily average dew point temperature or RHmax with minimum daily air temperature. In our case, we compared with RH_{max} data. The sensors used in the study are described in Table A1, Appendix A.

3. Methods

We followed the flowchart presented in Fig. 2. First, to estimate R_s (Section 3.1), we selected five different methods based on air temperature. These methods have adjustment coefficients that were calibrated and validated in order to obtain satisfactory performances. Prior to calibration, we performed a data preprocessing to capture all the temperature variability in the calibration and validation datasets. Then, we evaluated the ability of each method to simulate R_s in order to select the method with the best performance. Second, to estimate the VPD (Section 3.2.), we selected four different methods also based on air temperature. Then, we evaluated the ability of each method to estimate VPD in order to select the method with the best performance. Finally, with the methods selected previously, we evaluated the impact of R_s and VPD estimation on PM-ET_o calculation (Section 3.3). The methodological details are explained in the following subsections.
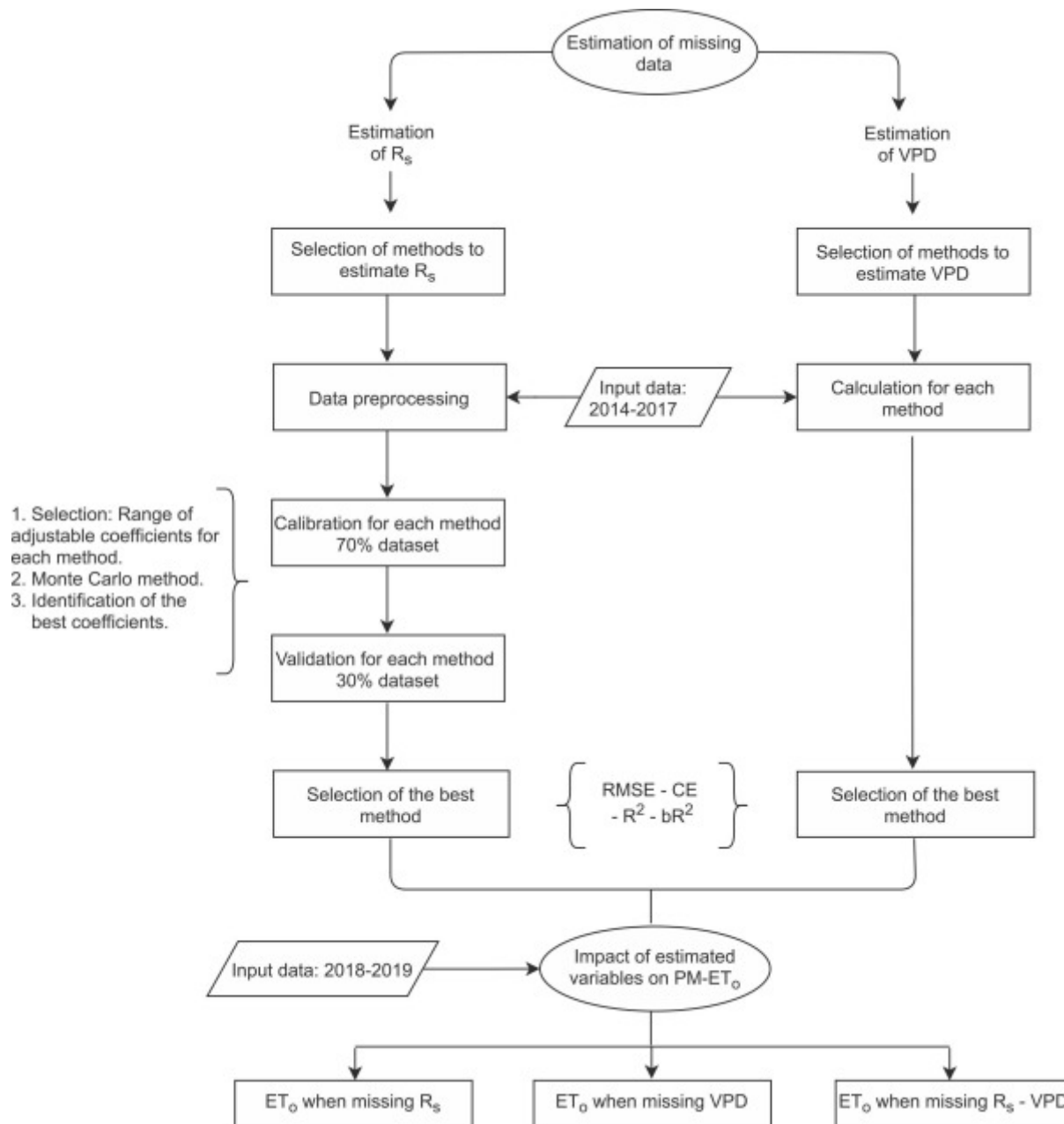
Download : Download high-res image (313KB)   Download : Download full-size image

Fig. 2. Flowchart of the PM-ET$_o$ calculation with estimation of R$_s$ and VPD.

3.1. Estimation of solar radiation

3.1.1. Methods to estimate R$_s$

Hargreaves and Samani (1982) – hereafter denoted as R$_s$-HS – recommended a method to estimate solar radiation using the difference between the maximum and minimum temperature. This is related to the degree of cloud cover in a given location:

$$R_s = K_{RS}\sqrt{T_{max} - T_{min}}\,R_a \tag{1}$$

where K_{RS} is an adjustment coefficient. The authors recommended K_{RS} values from 0.16 to 0.19, (0.16 for interior regions and 0.19 for coastal regions). R_a is extraterrestrial radiation (MJ m^{-2} day^{-1}) (Allen et al., 1998):

$$R_a = 37.6\,dr \quad (t.\sin\varphi.\sin\delta + \cos\varphi.\cos\delta.sint) \tag{2}$$

where dr is the reverse relative distance Earth-Sun (Eq. 3), t is the radiation angle at sunset (Eq. 4), δ is the solar decline (rad) (Eq. 5) and φ is the latitude of the location. J is the Julian day of the year (from 1 to 365 and from 1 to 366 for leap years):

$$dr = 1 + 0.033 \quad cos \quad (2\pi/365) \quad J \tag{3}$$

$$t = arcCos(-\tan\varphi.\tan\delta) \tag{4}$$

$$\delta = 0.4093 \quad sin \quad ((2\pi/365) \quad J - 1.39) \tag{5}$$

De Jong and Stewart (1993) – hereafter denoted as R$_s$-DS – suggested using the following equation incorporating precipitation and the range of daily temperature (ΔT):

$$R_s = \quad a * R_a * \quad (\Delta T)^b * \quad (1 + cp + dp^2 \quad) \tag{6}$$

where a, b, c and d are adjustment coefficients (Table A2, Appendix A see details of coefficients used by the authors), p is precipitation in mm, and ΔT can be calculated as:

$$\Delta T = \quad (T_{max}) - \frac{T_{min}(j) + \quad T_{min}(j+1)}{2} \tag{7}$$

where T_{max} in the daily maximum temperature (°C), $T_{min}(j)$ and $T_{min}(j+1)$ are the daily minimum temperature (°C) of the corresponding and the next day, respectively.

Allen (1995) – hereafter denoted as R$_s$-AL – modified Eq. 1 by estimating K_{RS} as a function of the ratio of atmospheric pressure:

$$k_{RS} = k_{RA}\left(\frac{P}{P_o}\right)^{0.5} \tag{8}$$

where k_{RA} is an adjustment coefficient having values in the 0.17–0.20 range, with values of 0.17 for inland regions and 0.20 for coastal regions; and P is the mean atmospheric pressure of the site (kPa); P_o is the mean atmospheric pressure at sea level (101.3 kPa):

$$P = P_0\left(\frac{293 - 0.0065Z}{293}\right)^{5.26} \tag{9}$$

where Z is the elevation (m a.s.l.) of the site.

Vanderlinden et al. (2004) – hereafter denoted as R$_s$-VA – found a relationship between the adjustment coefficient, k_{RS}, and the mean, minimum and maximum daily air temperatures:

$$k_{RS} = a * (\quad T_{mean}/TD) + b \tag{10}$$

where a and b are adjustment coefficients (Table A2, Appendix A see details of coefficients used by the authors), $T_{mean} = (T_{max} + T_{min})/2$ and $TD = T_{max} - T_{min}$.

Chen et al. (2004) – hereafter denoted as R_s-CH – found a logarithmic relationship between daily solar radiation, daily extra-terrestrial solar radiation, and the difference between the maximum and minimum daily air temperature:

$$R_s = a \; ln \; (T_{max} - T_{min}) - b * R_a \tag{11}$$

where a and b are adjustment coefficients (Table A2, Appendix A see details of coefficients used by the authors).

3.1.2. Data preprocessing

To avoid a bias in the selection of the samples for calibration and validation, we performed a data preprocessing. A duration curve was made for T_{max} - T_{min} (this variable serves as input for the aforementioned methods) for each weather station (Fig. 3). This analysis was made because, in preliminary calculations, random samples containing a disproportionately large percentage of high or low values caused a biased calibration of the methods (not shown). The curves showed inflection points around the 20th and the 90th percentiles in the three stations (limits indicated by the solid vertical lines in Fig. 3), which were set as the limits for the different groups of data. Therefore, the data was split into three sets: high values (≤20%), medium values (>20% and ≤90%) and low values (>90%) (Fig. 3). This data classification was subsequently used for assembling the groups for the calibration and validation processes (Section 3.1.3).
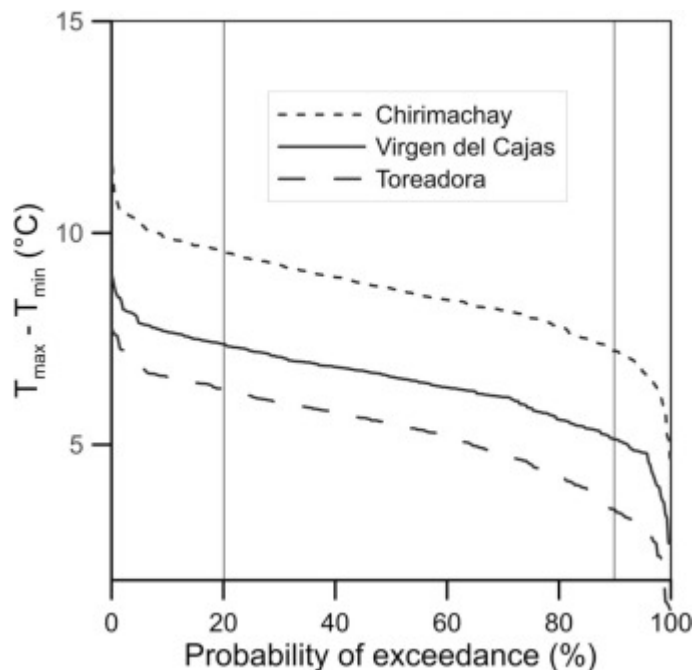
Fig. 3. Duration curve of the difference between the maximum and minimum daily air temperature by weather station.

3.1.3. Calibration and validation of Rs estimation methods

A model performs better when calibration is performed with a large dataset enough to contain a wide range of weather conditions (Motavita et al., 2019, Perrin et al., 2007, Xia et al., 2004). Motavita et al. (2019) also mentioned that in the calibration and validation datasets must contain a wide range of the variability. Bennett et al. (2013) suggested randomizing the division of data, so that the model performance is not biased by the allocation of data. Following these recommendations, we took the first 4 years of data for calibration and validation (2014–2017), and took 70% of the data for calibration, while 30% was left for validation. The calibration and validation samples were taken randomly but considering that each subset must fit the distribution criteria described in Section 3.1.2: 20% of high values, 70% of medium values, and 10% of low values.

In order to find a general method for the ecosystem, calibration was performed for the entire altitudinal gradient, by analyzing all data from the three weather stations combined as the methodology of De Jong and Stewart (1993) applied in their study. The Monte Carlo method was used to select the optimal coefficients after performing 5000 simulations. To calibrate each method, as a reference we started using the standard ranges of variation (Table A2, Appendix A). After previous calculations, we established our own ranges of variation because the ranges were widened or shortened (Table A3, Appendix A). Moreover, we validated each calibrated method with data independent of the calibration. After running the calibration and

validation for the altitudinal gradient, we applied the calibrated equations to the data set of each station using only 30% of validation data (as stated in Section 3.1.3).

3.2. Methods to estimate VPD

Vapor Pressure Deficit is estimated as the difference between the saturation vapor pressure, e_s, and the actual vapor pressure, e_a:

$$VPD = e_s - e_a \tag{12}$$

where e_s is calculated as:

$$e_s = \frac{e^\circ(T_{max}) + e^\circ(T_{min})}{2} \tag{13}$$

and when relative humidity data is available, e_a is calculated as:

$$e_a = \frac{e^\circ(T_{min})\frac{RH_{max}}{100} + e^\circ(T_{min})\frac{RH_{min}}{100}}{2} \tag{14}$$

where $e^\circ(T)$ is the saturation vapor pressure (kPa), and T_{max} and T_{min} are the maximum and minimum daily temperature (°C) and RH_{max} and RH_{min} are the maximum and minimum daily relative humidity. $e^\circ(T)$ for air temperature T is:

$$e^\circ(T) = 0.6108\, exp\left\lceil \frac{17.27*T}{T+237.3} \right\rceil \tag{15}$$

In the absence of humidity data, we evaluated four different methods based on air temperature to estimate the daily VPD, using four years of data (2014–2017).

In FAO56 Allen et al. (1998) – hereafter denoted as VPD-FAO – stated that e_a may be obtained by assuming that the dewpoint temperature, T_{dew}, is close to the T_{min}. The T_{dew} is usually experienced at sunrise in reference weather stations. In our study we do not have measures of T_{dew}, therefore we used T_{min} to estimate e_a. Due to the high humidity in our study area, the RH reaches 100% most of the night time hours, we found that using T_{min} between 05H00 and 08H00 to calculate e_a yielded better results than using absolute daily T_{min}:

$$e_a = e^\circ(T_{dew}) = 0.6108\, exp\left\lceil \frac{17.27*T_{dew}}{T_{dew}+237.3} \right\rceil \tag{16}$$

Doorenbos and Pruitt (1977) – hereafter denoted as VPD-DP – proposed the following method to estimate VPD:

$$VPD = e^\circ(T_{avg}) - e^\circ(T_{dew}) \tag{17}$$

where $e^\circ(T_{avg})$ is the saturation vapor pressure at the mean daily temperature.

Castellví et al. (1997) – hereafter denoted as VPD-CA1 – proposed the following method to estimate VPD:

$$VPD = e^\circ(T_a) - e^\circ(T_{dew}) \tag{18}$$

where T_a defined as the temperature that leaves equal areas under the curve $e°(T)-e°(T_{dew})$ between T_{max} and T_{min} using the trapezoidal method, for more detail review the research of Castellví et al. (1997).

Castellví et al. (1997) – hereafter denoted as VPD-CA2 – proposed the following method to estimate the mean relative humidity:

$$RH_{avg} = 100 * \frac{e°(T_{dew})}{\frac{1}{2}[e°(T_a)+e°(T_{avg})]} \tag{19}$$

then, we calculated e_a as proposed FAO56 (Allen et al., 1998):

$$e_a = \frac{RH_{avg}}{100}e°(T_{avg}) \tag{20}$$

3.3. Impact of R_s and VPD estimation on PM-ET_o calculation

We used two years of complete data (2018–2019) to calculate PM-ET_o, then we generated missing data scenarios by removing R_s or/and VPD values, and evaluated the impact on PM-ET_o calculation when these variables were estimated using the selected equations previously.

The PM-ET_o method defined by Allen et al. (1998) for calculating reference evapotranspiration of a hypothetical crop having a height of 0.12 m, a surface resistance of 70 s m^{-1} and an albedo of 0.23 is:

$$PM-ET_O = \frac{0.408\Delta(R_n-G)+y(900\quad/(T_{avg}\quad+273))u_2(e_s-e_a)}{\Delta+y(1+0.34u_2)} \tag{21}$$

where R_n is the net radiation at the crop surface (MJ m^{-2} day^{-1}), G is the soil heat flux density (MJ m^{-2} day^{-1}), T_{avg} at 2 m (°C), u_2 is the wind speed at 2 m (m s^{-1}), e_s is the saturation vapor pressure (kPa), e_a is the real vapor pressure (kPa), $e_s - e_a$ is the vapor pressure deficit (kPa), Δ is the slope of the vapor pressure curve (kPa °C^{-1}) and y is the psychrometric constant (kPa °C^{-1}). For daily computations, G equals zero as the magnitude of daily soil heat flux beneath the grass reference surface is very small (Allen et al., 1998).

3.4. Evaluation criteria

The statistical indices used to evaluate the methods performance were: i) the Nash–Sutcliffe efficiency (CE), which has been widely used to evaluate the performance of empirical models and it is sensitive to differences in the observed and simulated means and variances; ii) the coefficient of determination (R^2), which describes how much of the observed dispersion is explained by the prediction; iii) the coefficient of determination multiplied by the slope, b (br^2), a model which systematically over- or underpredicts all the time will still result in good R^2 values close to 1.0 even if all predictions were wrong. Therefore, is advisable to take into account additional information which can cope with that problem. This information is provided by the slope b and as long as b is close to one, is better and, iv) the root mean square error $(RMSE)$, which is a weighted measure of the error in which the largest deviations between the observed and modeled values contribute the most (Table A4, Appendix A). To

evaluate the quality of the PM-ET$_o$ calculations when one or two variables were missing, we used the same statistical indices.

4. Results and discussion

4.1. Estimation of solar radiation

To estimate solar radiation, we used a period data 2014–2017. In the absence of R$_s$ observations, this variable was estimated using methods based on air temperature with locally calibrated adjustment coefficients ((1), (2), (3), (4), (5), (6), (7), (8), (9), (10), (11)). Table 2 shows the coefficients and statistical indicators of the calibration of the methods to estimate R$_s$.

Table 2. Adjustment coefficients and statistics of the calibration of the methods to estimate daily R$_s$ in the altitudinal gradient. (70% of data set - period 2014–2017).

Method	K$_{RS}$	K$_{ra}$	a	b	c	d	RMSE (MJ m^{-2} day^{-1})	CE	R^2	bR^2
R$_s$-HS	0.1094	–	–	–	–	–	3.58	0.47	0.51	0.47
R$_s$-DS	–	–	0.5025	0.6879	-0.0350	0.0014	3.28	0.55	0.57	0.53
R$_s$-AL	–	0.1376	–	–	–	–	3.58	0.47	0.51	0.47
R$_s$-VA	–	–	0.0045	0.1020	–	–	3.73	0.42	0.50	0.47
R$_s$-CH	–	–	0.1536	-0.4475	–	–	3.63	0.45	0.47	0.43

When we combined the data from the three stations to calibrate the methods and to select the best method for the gradient, it was found that the adjustment coefficients of each method varied from their original values. In a global context, the difference of the coefficients is related to the different climatic regions where the methods have been developed and tested. These methods have been mostly applied in arid and semi-arid regions, and to a lesser degree in humid regions. In the available literature in sub-humid and humid regions it was found that to estimate R$_s$, the authors commonly use the recommendations of Allen (1995) and Hargreaves and Samani (1982) with a local calibration of the k$_{RS}$ coefficient (Jabloun and Sahli, 2008, Paredes et al., 2020, Paredes et al., 2017, Paredes and Pereira, 2019). In such studies, the values of k$_{RS}$ coefficient were higher for both methods (R$_s$-HS and R$_s$-AL) compared to the k$_{RS}$ values in our study area. The variability of the coefficients is influenced by the change in the Diurnal Temperature Range (DTR), where the DTR decreases as altitude increases, as confirmed by Córdova et al. (2015) for our study area. Liu et al. (2009) found that *a* increases as altitude increases and the DTR decreases, and the opposite was found for *b*: it decreases as

altitude increases and the DTR decreases. This relation between the coefficients for this method and altitude was also found by Li et al. (2013).

The Rs-CH method showed values in the range of 0.16–0.42 (coefficient *a*) and –0.45–0.12 (coefficient *b*) in the North China Plain Chen et al. (2004). In our case, the calibration had lower values but with similar behavior. At higher altitudes, the coefficient *a* increases and the coefficient *b* decreases. The R_s-VA method showed average values of 0.0030 and 0.0022 for the coefficients *a* and *b*, respectively, in Southern Spain (Vanderlinden et al., 2004), while we found higher values in our study. In the R_s-DS method, the values of the coefficients *a* (0.127), *b* (0.599), *c* (–0.028) and *d* (0.0003) reported in western Canada (De Jong and Stewart, 1993) were similar to our values, except by the coefficient *a* that was greater. For a detailed comparison of coefficients, see Table 2. The table shows that the changes in the coefficients of the five methods are study area-dependent due to the use of local data bases.

The methods that use DTR as input (R_s-HS, R_s-AL, R_s-VA, and R_s-CH) had similar performance, showing a <u>RMSE</u> in the range from 3.58 to 3.73 MJ m^{-2} day^{-1}, a CE from 0.42 to 0.47, and R^2 and bR^2 values from 0.47 to 51 and from 0.43 to 0.47, respectively. Whereas the R_s-DS method that used $\triangle$T and the effect of precipitation ((6), (7)), yielded better estimations than the other methods with higher values of CE, R^2, and bR^2, and a lower value of RMSE (Table 2). Especially in humid regions, the use of precipitation has a considerable effect on solar radiation reducing the solar <u>transmissivity</u> due to the presence of cloud.

Table 3 presents the results of the validation for the methods in the altitudinal gradient. It was observed that the performance of the R_s-HS, R_s-AL, R_s-VA and R_s-CH methods was similar to the calibration performance, and it was confirmed that R_s-DS method is the highest performing one.

Table 3. Statistics of the validation of the methods to estimate daily R_s in the altitudinal gradient. (30% of data set - period 2014–2017).

Method	RMSE (MJ m^{-2} day^{-1})	CE	R^2	bR^2
R_s-HS	3.61	0.48	0.53	0.48
R_s-DS	3.42	0.53	0.54	0.50
R_s-AL	3.62	0.47	0.53	0.47
R_s-VA	3.76	0.43	0.52	0.47
R_s-CH	3.65	0.46	0.49	0.44

Once the methods were calibrated for the gradient, we evaluated them using the data from each station individually. The scatter plot for Chirimachay (Fig. 4a,d,g,j,m) showed high

dispersion and slight overestimation for R_s below 15 MJ m^{-2} day^{-1}. This was reflected in a slight increase in RMSE and a lower CE compared to the results obtained for the entire gradient. Moreover, the R_s-DS and R_s-AL methods showed the best results, a lower RMSE and a higher CE, R^2 and bR^2. However, these results did not differ greatly from the performance of the rest of the methods at the site (Table 4).
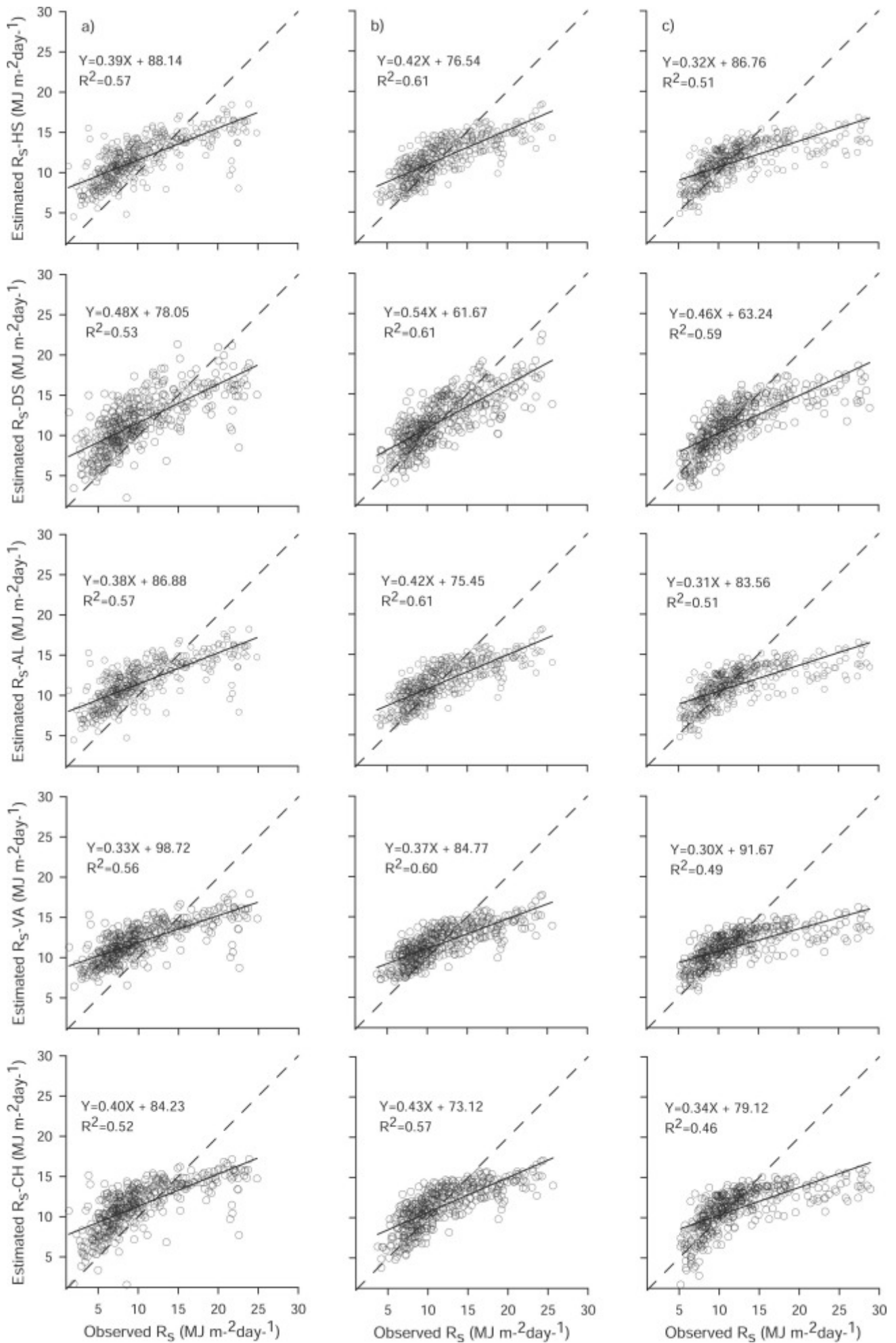
Fig. 4. Comparison of daily R_s observed and estimated (with five methods) in all stations (Chirimachay, Virgen and Toreadora). These results correspond to 30% of data set used for validation. The solid line represents the fitted regression line. The dashed line indicates 1:1.

Table 4. Statistics used to evaluate the performance of the calibrated methods to estimate daily R_s in the data of each site. (30% of data set used for validation).

Station	Methods	RMSE (MJ m^{-2} day^{-1})	CE	R^2	bR^2
Chirimachay	R_s-HS	3.84	0.43	0.57	0.56
	R_s-DS	3.81	0.44	0.53	0.52
	R_s-AL	3.79	0.44	0.57	0.56
	R_s-VA	4.11	0.34	0.56	0.55
	R_s-CH	3.82	0.43	0.52	0.50
Virgen	R_s-HS	3.05	0.55	0.61	0.56
	R_s-DS	2.89	0.60	0.61	0.57
	R_s-AL	3.07	0.55	0.61	0.55
	R_s-VA	3.19	0.51	0.60	0.55
	R_s-CH	3.11	0.54	0.57	0.52
Toreadora	R_s-HS	3.91	0.41	0.51	0.42
	R_s-DS	3.52	0.52	0.59	0.50
	R_s-AL	3.96	0.39	0.51	0.42
	R_s-VA	4.03	0.37	0.49	0.41
	R_s-CH	3.99	0.38	0.46	0.38

We found that Virgen had the best adjustment to the observed values in all the methods in comparison to the other sites, and the method with the best performance was R_s-DS (Table 4; Fig. 4b,e,h,k,n). In Toreadora, the CE presented the lowest values compared to the other sites for all the methods except for R_s-DS. This method showed the best performance to estimate R_s at the site (Table 4).

At the Virgen site, where the methods showed the best results, we hypothesize that this could be because of two reasons. Firstly, the methods for estimating ET_o were mainly developed in

arid and semiarid regions, thus the site with the lowest RH (which is Virgen) might show the best results. And secondly, the more <u>stable boundary layer</u> in Virgen related to the local relatively flatter topography of the site provides the conditions for air temperature to be more related to R_s compared to the other sites, which in the end will yield better results when R_s is estimated from temperature measurements.

In addition, we found that the ability of the methods to estimate R_s is affected by elevation, because there is a major incidence of solar radiation in high areas; but such effect on the temperature is low. This is due to the fact that only a small fraction of R_s is absorbed by the thinner atmosphere of these high elevation sites (Llambí et al., 2012). This means that the incoming R_s does not heat up, and this is reflected in the underestimation of high values of R_s. Therefore, at the highest site, Toreadora, the highest values of R_s resulted in the lowest accuracy ($bR^2 < 0.51$) in all methods compared to the other sites. At this location, the methods that used DTR (R_s-HS, R_s-AL, R_s-VA and R_s-CH) estimated R_s values up to 15 MJ m^{-2} day^{-1} (80% of data) and the R_s-DS method (which uses ΔT and the effect of precipitation) estimated R_s values up to 19 MJ m^{-2} day^{-1} (90% of data). While for the Chirimachay and Virgen sites, the R_s-HS, R_s-AL, R_s-VA and R_s-CH methods presented difficulty in estimating $R_s > 17$ MJ m^{-2} day^{-1} (12.86% of data), and the R_s-DS method estimated R_s values up to 21 MJ m^{-2} day^{-1} (93.24% of data) (Fig. 4).

The performance of the methods based on temperature increases as DTR increases (Allen, 1997, Li et al., 2014, Samani, 2000). Therefore, this performance decreases with the altitude, because DTR is reduced. Evidently, our results agree with this elevation effect that causes DTR to decrease in the highest site. This finding is also consistent with the results presented by Paredes et al. (2017). In sites with higher elevation, the DTR was lower and the extreme values were not well estimated. As well as Li et al. (2014) in China and Bandyopadhyay et al. (2008) in India, who reported the failure of these methods for high elevation stations, both studies estimated monthly solar radiation.

4.2. Estimation of vapor pressure deficit

To estimate vapor pressure deficit, we used a period data 2014–2017. Table 5 summarizes the statistical indicators of the methods applied to estimate daily VPD. It was found that in the gradient the RMSE was in the range from 0.08 to 0.30 kPa, the CE with values between 0.24 and 0.63, the R^2 with values between 0.55 a 0.81, and bR^2 from 0.35 to 0.71. The VPD-FAO method had the highest performance in most of the statistical indicators, but also showed a slight overestimation for low and medium values. In addition, an underestimation of low values was found using the VPD-DP, VPD-CA1 and VPD-CA2 methods in Chirimachay and an overestimation of medium values by the VPD-CA1 and VPD-CA2 methods in Virgen and Toreadora (Fig. 5).

Table 5. Statistics used to evaluate the performance of the methods to estimate daily VPD in the data of each site. Complete data set - Period 2014–2017.

Station	Methods	RMSE (kPa)	CE	R^2	bR^2
Chirimachay	VPD-FAO	0.12	0.40	0.81	0.64
	VPD-DP	0.11	0.47	0.55	0.43
	VPD-CA1	0.30	0.32	0.58	0.43
	VPD-CA2	0.12	0.39	0.76	0.70
Virgen	VPD-FAO	0.08	0.63	0.80	0.70
	VPD-DP	0.10	0.39	0.61	0.45
	VPD-CA1	0.08	0.62	0.74	0.68
	VPD-CA2	0.1	0.30	0.79	0.62
Toreadora	VPD-FAO	0.09	0.62	0.77	0.71
	VPD-DP	0.13	0.21	0.63	0.35
	VPD-CA1	0.10	0.63	0.73	0.69
	VPD-CA2	0.13	0.24	0.75	0.59
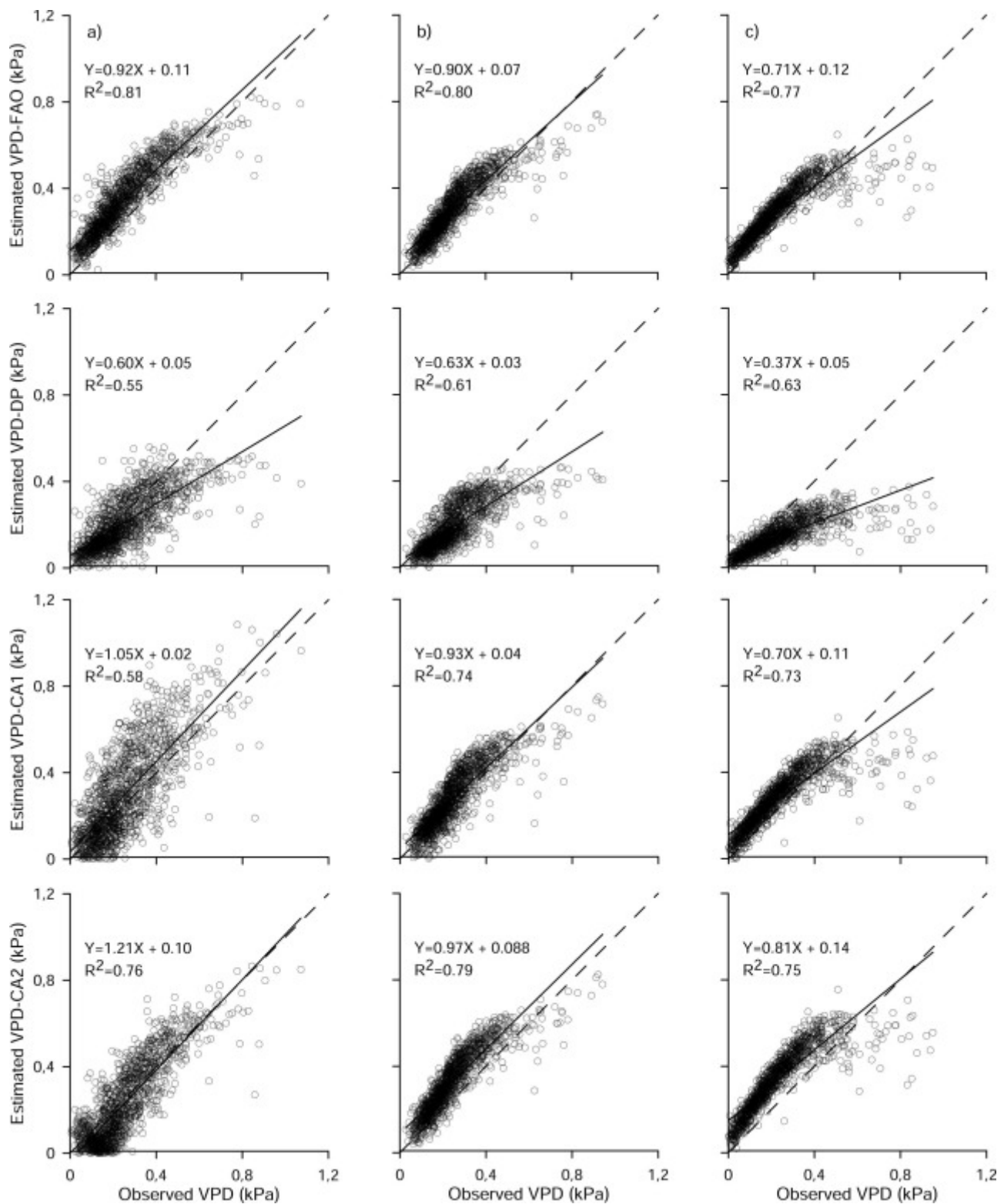
Fig. 5. Comparison of daily observed and estimated VPD (with four methods) in all stations (Chirimachay, Virgen and Toreadora). Period 2014–2017. The solid line represents the fitted regression line. The dashed line indicates 1:1.

To find the best method for the gradient, we analyzed the statistics site by site. In Chirimachay, the VPD-FAO method had the best performance with the highest R^2 and bR^2

and a low RMSE (0.12 kPa). In Virgen and Toreadora the VPD-FAO method had the lowest RMSE with values of 0.08 and 0.09 kPa, respectively. The other statistical results confirmed that the VPD-FAO method had the highest performance (Table 5).

Therefore, we conclude that the VPD-FAO method is the most suitable method to estimate VPD in the altitudinal gradient. However, the overestimation presented by this approach has also been found in other studies performed in humid climates (Landeras et al., 2008, Paredes et al., 2017, Todorovic et al., 2013, Tomas-Burguera et al., 2017). This could be due to the fact that $T_{dew} > T_{min}$ in sub-humid and humid climates (Paredes et al., 2017, Todorovic et al., 2013). Hence, by assuming $T_{dew} = T_{min}$, e_a is being underestimated and therefore VPD is overestimated. In fact, a previous analysis showed that when we took the daily minimum temperature the overestimation was 0.04 kPa per day greater than the current one. To decrease this overestimation, we took the minimum temperature at sunrise (05H00 – 08H00) to get closer to the actual value of T_{dew}.

## 4.3. Estimation of daily ET_o when R_s and /or VPD are missing (period 2018–2019)

Table 6 shows the statistical performance of the PM-ET_o calculation when R_s and/or VPD were missing and were estimated with the best methods selected for the altitudinal gradient. It was found that the PM-ET_o calculation results were worse when the missing variable was R_s, while when VPD data were missing, the PM-ET_o estimates were closer to the PM-ET_o values calculated with the complete data set. This is evident in all statistical indicators with the lowest RMSE and the highest CE, R^2 and bR^2. As expected, the largest error occurred when data for two variables were missing and their values were estimated (Table 6).

Table 6. Comparison between daily PM-ET_o calculated with full data set and daily PM-ET_o calculated when R_s and/or VPD were missing and were estimated with the best methods (R_s-DS and VPD-FAO). Period 2018–2019.

Station	PM-ET_o	RMSE (mm day^{-1})	CE	R^2	bR^2
Chirimachay	R_s-DS	0.33	0.79	0.85	0.82
	VPD-FAO	0.16	0.95	0.99	0.93
	R_s-DS and VPD-FAO	0.42	0.66	0.83	0.75
Virgen	R_s-DS	0.29	0.81	0.83	0.79
	VPO-FAO	0.12	0.97	0.98	0.95
	R_s-DS and VPD-FAO	0.32	0.77	0.78	0.77

Station	PM-ET$_o$	RMSE (mm day^{-1})	CE	R^2	bR^2
Toreadora	R$_s$-DS	0.27	0.86	0.89	0.83
	VPD-FAO	0.18	0.94	0.97	0.94
	R$_s$-DS and VPD-FAO	0.34	0.79	0.82	0.80

The site by site analysis showed that the high ET$_o$ values were underestimated in Chirimachay, Virgen, and Toreadora, and only in Chirimachay a slight overestimation of the lower values existed on PM-ET$_o$ calculation with estimated R$_s$. This behavior is well explained by the relationships between R$_s$-DS and observed R$_s$, above previously analyzed (Fig. 4a-o). The estimated values of PM-ET$_o$ R$_s$-DS were better than R$_s$-DS estimates. The good relationship between PM-ET$_o$ and PM-ET$_o$ R$_s$-DS is highlighted in Fig. 6a-c and Table 6, with R^2 > 0.82 and bR^2 > 78 in the three sites. Moreover, the RMSE values were below 0.34 mm day^{-1}, and the highest performance was found in Toreadora (Table 6; Fig. 6c).
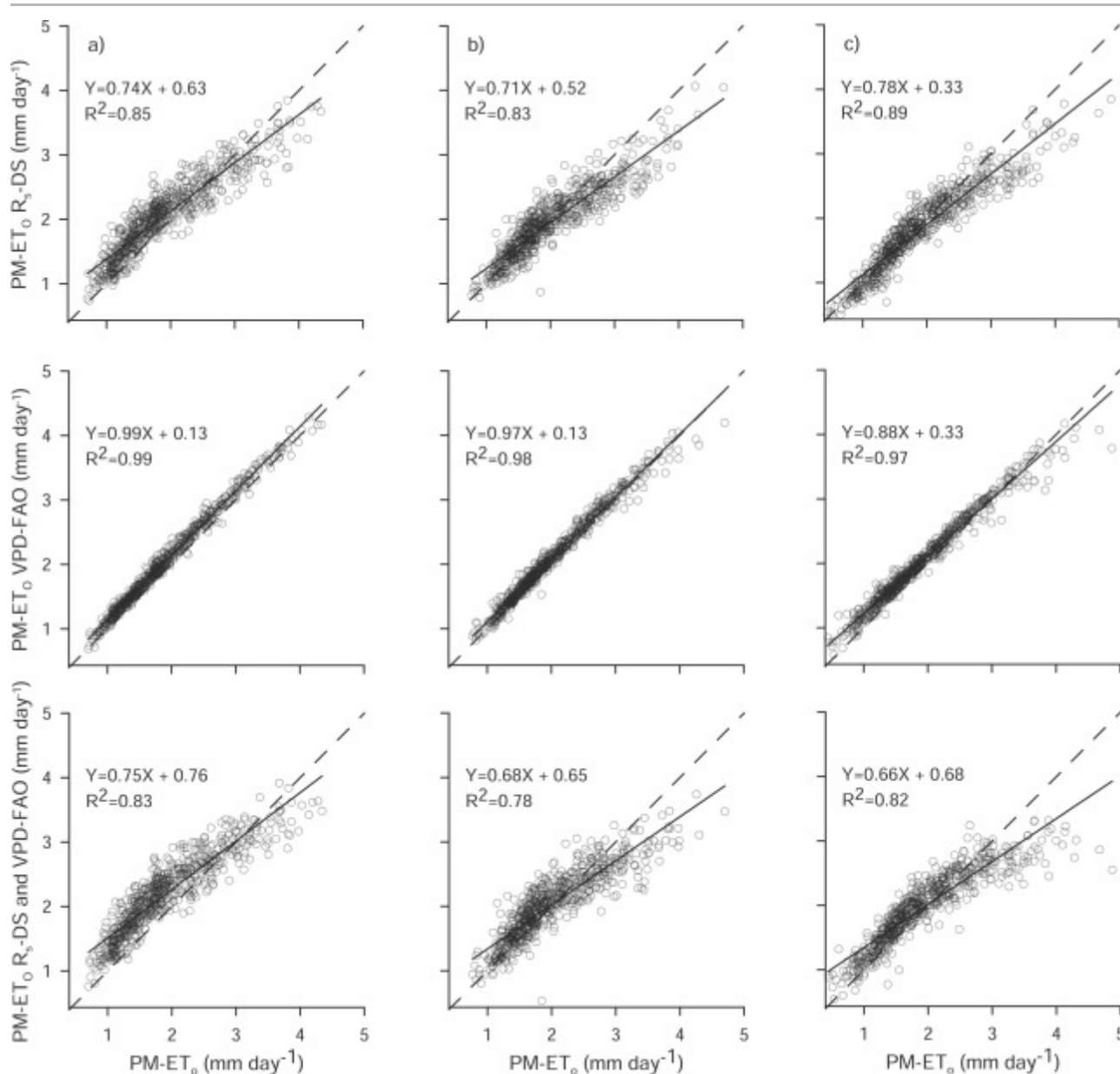
Download : Download high-res image (605KB)   Download : Download full-size image

Fig. 6. Comparison of daily PM-ET$_o$ and PM-ET$_o$ R$_s$-DS and/or VPD-FAO in all stations: Chirimachay, Virgen and Toreadora. Period 2018–2019. The solid line represents the fitted regression line. The dashed line indicates 1:1.

The novelty of our results lies in the fact that limited information is available on this topic for humid conditions, and there is only one previous study which preliminary explored the topic in the high Tropical Andes (Córdova et al., 2015). Such investigation concluded that for the PM-ET$_o$ calculation, the observations of R$_s$ are extremely important in this area, because when this variable was missing, and it was estimated without local calibration, the ET$_o$ yielded the maximum error (RMSE of 0.53 mm day $^{-1}$). In contrast, our results showed a decrease in the RMSE to 0.27 mm day $^{-1}$, after selecting the best method to estimate R$_s$ in this zone. The research of Souza et al. (2016) had similar findings in humid conditions in the Mato Grosso State: among the methods used to estimate R$_s$, the method proposed by De Jong and Stewart (1993) resulted in the lowest RMSE on PM-ET$_o$ calculations.

Previous studies, developed under humid conditions, have reported an underestimation of high values and a slight overestimation of low values on ET$_o$ calculation, when R$_s$ was estimated. In this case, using the method of Hargreaves and Samani (1982) with the locally calibrated K$_{RS}$ coefficient (Paredes et al., 2017, Paredes and Pereira, 2019). Paredes et al. (2020) in their study computed k$_{RS}$ using a trial and error procedure and k$_{RS}$ as a function of T$_{max}$ - T$_{min}$, RH and u$_2$. in a global equation and equations focused on climatic conditions. In humid conditions, in all cases an RMSE was found between 0.54 and 0.61 mm day^{-1}.

The analysis of the results between PM-ET$_o$ and PM-ET$_o$ VPD-FAO indicated that when e$_a$ data were estimated (assuming T$_{dew}$ = T$_{min}$ to determine VPD), the calculations had a very high performance in the altitudinal gradient. The R^2 values exceeded 0.96 and the bR^2 values exceeded 0.92. The lowest values of RMSE (< 0.19 mm day^{-1}) were supported by the high CE from 0.94 to 0.97 (Table 6). These outcomes corroborate the findings of the previous work of Córdova et al. (2015), who found that the ET$_o$ calculation using VPD-FAO method had a RMSE of 0.17 mm day^{-1} in Toreadora. Despite the good performance, the PM-ET$_o$ VPD-FAO calculation showed a slight tendency to overestimate low and medium values. This finding broadly supports the work of other studies in humid conditions. For example, the work of Sentelhas et al. (2010) in Canada and Landeras et al. (2008) in Northern Spain found the ET$_o$ was overestimated when the VPD-FAO method was applied assuming T$_{dew}$ = T$_{min}$ to calculate e$_a$ when relative humidity data is missing. Also, the study of Garcia et al. (2004) in the Bolivian highlands showed the ET$_o$ calculation with a RMSE of 0.2 mm day^{-1} when RH data is missing and they used the VPD-FAO method to estimate the variable.

As reviewed before, numerous studies assumed T$_{dew}$ = T$_{min}$ and reported good results of using Eq. (16) in humid conditions. However, it was also found in other studies carried out in a wide variety of climates that use a correction (aridity index) to improve the estimation of T$_{dew}$ such as T$_{dew}$ = T$_{mean}$-a$_D$. For example, Todorovic et al. (2013) and Raziei and Pereira (2013) in humid conditions, the estimation of ET$_o$ showed a RMSE (0.36 and 0.19 mm day^{-1}) higher than our

results. Paredes et al. (2017) in the humid conditions of Azores islands also applied an adjustment in T_{dew} estimations, in this case the adjustment was for winter and summer season. The results of ET_o showed a slight overestimation and a RMSE between 0.48 and 0.15 mm day^{-1}. Paredes et al. (2020) in their study showed that when they apply the correction in the estimation of T_{dew}, the ET_o calculation increases their performance with a RMSE between 0.19 and 0.32 mm day^{-1}. In all studies, error increases for semi-arid to hyper-arid conditions.

As expected, the largest error occurred when both R_s-DS and VPD-FAO were used to estimate PM-ET_o instead of observations. Overall, in the altitudinal gradient, an increase in RMSE (> 0.32 mm day^{-1}) was observed, and the over and under estimation of both variables was reflected in a CE between 0.66 and 0.79. The good correlation between observed and estimated values was reflected by $R^2 > 0.77$ and $bR^2 > 0.74$ (Table 6, Fig. 6g,h,i). These findings are consistent with those of Landeras et al. (2008) in Northern Spain, and Sentelhas et al. (2010) in Canada. Paredes et al. (2020) in climate types - humid, sub-humid, semi-arid, and hyper-arid and arid. Where the error increment on ET_o calculation when R_s and RH data were missing.

In our study area, the estimates of R_s were less precise than VPD, and these observations were also reflected on PM-ET_o calculation. The underestimation of high ET_o values that was found when estimating R_s, was also evident in the calculation of PM-ET_o R_s-DS and VPD-FAO. Moreover, the tendency to overestimate low and medium values shown on PM-ET_o VPD-FAO calculation was also observed in the calculation of PM-ET_o R_s-DS and VPD-FAO. Despite this over-or under-estimation, the RMSE was low: 0.42, 0.32 and 0.34 mm day^{-1} for Chirimachay, Virgen, and Toreadora, respectively compared to the results reported by Córdova et al. (2015). They found a RMSE 0.71 mm day^{-1} in the Toreadora site when R_s and HR data were missing, using the recommendations of Hargreaves and Samani (1982) and Allen (1995)). Hence, the calculation of ET_o with the PM method when R_s and/or VPD were missing and were estimated with the R_s-DS and VPD-FAO methods was reliable in our study area.

Recent approaches have proposed an alternative solution to estimate ET_o when the weather data sets are not available using remotely sensed or reanalysis data. For example; Paredes et al. (2021) from a variety of climate conditions evaluated the usability of the LSA-SAF and ERA5 products provided by the Meteosat Second Generation (MSG) Geostationary satellite for ET_o estimation. The results of the comparison the R_s LSA-SAF estimates with R_s ground data showed a good correspondence between the two data sets for continental Portugal, but a tendency for Rs LSA-SAF to underestimate the R_s ground in the cloudy islands of the Azores. It was observed that ET_o calculated with data from R_s LSA-SAF and observed T, RH and U_2 is strongly correlated with PM-ET_o ($R^2 > 0.97$) for most places in continental Portugal. For most of the Azores locations, ET_o LSA-SAF overestimated PM-ET_o. The R_s data from the ERA5 reanalysis showed a similar behavior to that of the LSA-SA products.

Ishak et al. (2010) explored a potential application of reduced-scale global reanalysis meteorological data using the Mesoscale Modeling System 5 (MM5). The ERA-40 reanalysis data are downscaled to the Brue catchment in southwest England. When comparing with observed data, the atmospheric pressure could be derived very precisely with an error less

than 0.2%, the error in u_2 from 200% to 400%, T (<10%), RH (5–21%) and R_s (4–23%). The downscaling process improved data quality (except u_2) However, ET_o values were significantly overestimated according to the FAO Penman-Monteith equation.

Blanco et al. (2015) developed a new approach that considers a modified version of the Makkink equation and is based on a combination of remote sensing Rs considering the MSG satellite and a numerical weather forecast of near-surface air temperature (T2m). The new approach provided accurate daily estimates of ET_o compared to lysimeter data (RMSE 0.50 mm d^{-1}). In addition, the approach allowed ET_o assessment on a regional scale, it is especially useful for those areas with missing or meteorological in situ observations.

5. Conclusions

The objective of this investigation was to assess the impact on PM-ET_o calculation when solar radiation (R_s) and/or vapor pressure deficit (VPD) were missing in the high Tropical Andes (humid páramo, 3298–3955 m a.s.l.). Here, continuous high quality meteorological data are not available, or time series are incomplete. This study is the first in the region to evaluate nine methods to estimate R_s and VPD – based on daily maximum and minimum temperature – and to evaluate their impact on PM-ET_o calculation.

The first finding has shown that the calibration and validation of methods to calculate R_s was essential to obtain more accurate R_s estimations for this ecosystem. The R_s-DS method had the highest performance in our study area, an RMSE between 2.89 and 3.81 MJ m^{-2} day^{-1} and R^2 > 0.52. Despite an underestimation of values above 19 MJ m^{-2} day^{-1}, the R_s-DS method seems to be a feasible approach to estimate the missing variable.

The second finding has shown that the VPD-FAO method had the highest performance out of the 4 methods evaluated to estimate VPD in all statistical indicators used: RMSE between 0.08 and 0.12 kPa and R^2 > 0.76. Therefore, in the absence of RH observations, the use of T_{dew} = T_{min} could be an excellent alternative to estimate e_a in the páramo ecosystem with a slight overestimation for low and medium values.

Finally, the results of this investigation showed that because of the fact that we properly estimated R_s and VPD, the calculation of PM-ET_o presented good statistical indicators. When only R_s is missing, PM-ET_o had an RMSE between 0.29 and 0.34 mm day^{-1} and R^2 > 0.82; when only VPD is missing, PM-ET_o had an RMSE between 0.12 and 0.18 mm day^{-1} and R^2 > 0.96. As expected, when both variables were missing, the ET_o calculation increased its error, an RMSE between 0.32 and 0.42 mm day^{-1} and R^2 > 0.77. We conclude that the calculation of ET_o with the PM method when R_s and/or VPD were missing and were estimated with the R_s-DS and VPD-FAO methods was reliable in our area.

Results obtained in the current study have shown that the calibration of equations to estimate missing variables (R_s and/or RH) provides a solution to calculate reliable PM-ET_o in the páramo ecosystem when aiming at improved water productivity for domestic and industrial uses, irrigated agriculture, and hydropower. Moreover, the procedures herein assessed can be

used for other humid locations, considering that the adjustment coefficients should be locally calibrated.

Declaration of Competing Interest

The authors declare that they have no known competing financial interests or personal relationships that could have appeared to influence the work reported in this paper.

Acknowledgments

Appendix A.

(see Table A1, Table A2, Table A3, Table A4).

Table A1. Details of the sensors.

Variable	Sensor Type	Unit	Accuracy	Time Resolution
Air temperature / Relative Humidity	Campbell CS-215 + Radiation Shield	°C/%RH	± 0.3 °C/ ± 2% RH	5 min
Solar Radiation	Campbell CS300 Pyranometer	$W\ m^{-2}$	± 5% daily total	5 min
Wind Speed and Direction	Met-One 034B Wind Set	$m\ s^{-1}$	± 0.11 $m\ s^{-1}$	5 min

Table A2. Range of the adjustable coefficients selected from literature.

Methods	K_{RS}	K_{ra}	a	b	c	d
R_s-HS	0.16–0.19	–	–	–	–	–
R_s-DS	–	–	0.11–0.51	0.08–0.64	-0.03–0.02	0.0003–0.009
R_s-AL	–	0.17–0.20	–	–	–	–
R_s-VA	–	–	0.003–0.06	0.002–0.06	–	–
R_s-CH	–	–	0.16–0.42	-0.45–0.12	–	–

Table A3. Range of the adjustable coefficients of each method of the present study.

Methods	K_{RS}	K_{ra}	a	b	c	d
R_s-HS	0.096–0.12	–	–	–	–	–
R_s-DS	–	–	0.48–0.52	0.65–0.80	-0.03–0.017	0.0009–0.004
R_s-AL	–	0.10–0.15	–	–	–	–
R_s-VA	–	–	0.045–0.1	0.01–0.03	–	–
R_s-CH	–	–	0.149–0.159	-0.47–0.3	–	–

Table A4. Performance evaluation criteria.

Criteria	Equation	Optimal value
Nash–Sutcliffe efficiency	$CE = 1 - \dfrac{\Sigma_{i=1}^{n}(x_i - x_o)}{\Sigma_{i=1}^{n}(x_o - \underline{x_o})}$	1
Coefficient of determination	$R^2 = \dfrac{\Sigma_{i=1}^{n}\left(x_i - \underline{x_o}\right)^2}{\Sigma_{i=1}^{n}\left(x_o - \underline{x_o}\right)^2}$	1
Coefficient of determination multiplied by the slope	$br^2 = |b|R^2, b \leq 1; br^2 = \dfrac{R^2}{|b|}, b > 1$	1
Root mean square error	$RMSE = \sqrt{\dfrac{1}{n}\Sigma_{i=1}^{n}(x_i - x_o)^2}$	0

Where x_i is the estimated value; x_o is the observed value; n is the number of observations and $\underline{x_o}$ is the mean of the observed values; b in the slope.

Recommended articles

References

Allen, 1995   R. Allen
Evaluation of procedures for estimating mean monthly solar radiation from air temperature
J. Hydrol. Eng., 2 (1995), pp. 56-67
    View Record in Scopus   Google Scholar

Allen, 1997   R.G. Allen
Self-calibrating method for estimating solar radiation from air temperature
J. Hydrol. Eng., 2 (1997), pp. 56-67, 10.1061/(asce)1084-0699(1997)2:2(56)
    View Record in Scopus   Google Scholar

Allen et al., 1998   Allen, R.G., Pereira, L.S., Raes, D., Smith, M., Ab, W., 1998. Fao,1998. Irrig. Drain. Pap. No. 56, FAO 300. https://doi.org/10.1016/j.eja.2010.12.001.
Google Scholar

Bandyopadhyay et al., 2008   A. Bandyopadhyay, A. Bhadra, N.S. Raghuwanshi, R. Singh
Estimation of monthly solar radiation from measured air temperature extremes
Agric. Meteorol., 148 (2008), pp. 1707-1718, 10.1016/j.agrformet.2008.06.002
Article   🗎 Download PDF   View Record in Scopus   Google Scholar

Beck et al., 2008   Beck, E., Bendix, J., Kottke, I., Makeschin, F., Mosandl, R., 2008. The Ecosystem (Reserva Biológica San Francisco) In: Beck, Erwin Bendix, Jörg Kottke, Ingrid Makeschin, Franz Mosandl, Reinhard Gradients in a Tropical Mountain Ecosystem of Ecuador. Ecological Studies, 198.
Google Scholar

Bennett et al., 2013   N.D. Bennett, B.F. Croke, G. Guariso, J.H. Guillaume, S.H. Hamilton, A.J. Jakeman, S. Marsili-Libelli, L.T. Newham, J.P. Norton, C. Perrin, S.A. Pierce, B. Robson, R. Seppelt, A.A. Voinov, B.D. Fath, V. Andreassian, C. Land
Characterising performance of environmental models q
Environ. Model. Softw., 40 (2013), pp. 1-20, 10.1016/j.envsoft.2012.09.011
Article   🗎 Download PDF   View Record in Scopus   Google Scholar

Berndt and Haberlandt, 2018   C. Berndt, U. Haberlandt
Spatial interpolation of climate variables in Northern Germany—influence of temporal resolution and network density
J. Hydrol. Reg. Stud., 15 (2018), pp. 184-202, 10.1016/j.ejrh.2018.02.002

Article   📄 Download PDF   View Record in Scopus   Google Scholar

Besharat et al., 2013   F. Besharat, A.A. Dehghan, A.R. Faghih
Empirical models for estimating global solar radiation: a review and case study
Renew. Sustain. Energy Rev., 21 (2013), pp. 798-821, 10.1016/j.rser.2012.12.043
Article   📄 Download PDF   View Record in Scopus   Google Scholar

Buytaert et al., 2006   W. Buytaert, R. Célleri, B. De Bièvre, F. Cisneros, G. Wyseure, J. Deckers, R. Hofstede
Human impact on the hydrology of the Andean páramos
Earth Sci. Rev., 79 (2006), pp. 53-72, 10.1016/j.earscirev.2006.06.002
Article   📄 Download PDF   View Record in Scopus   Google Scholar

Carrillo-Rojas et al., 2016   G. Carrillo-Rojas, B. Silva, M. Córdova, R. Célleri, J. Bendix
Dynamic mapping of evapotranspiration using an energy balance-based model over an andean páramo catchment of southern ecuador
Remote Sens. (2016), p. 8, 10.3390/rs8020160
Google Scholar

Castellví et al., 1997   F. Castellví, P.J. Perez, C.O. Stockle, M. Ibañez
Methods for estimating vapor pressure deficit at a regional scale depending on data availability
Agric. . Meteorol., 87 (1997), pp. 243-252, 10.1016/S0168-1923(97)00034-8
Article   📄 Download PDF   View Record in Scopus   Google Scholar

Célleri and Feyen, 2009   R. Célleri, J. Feyen
The hydrology of tropical andean ecosystems: importance, knowledge status, and perspectives
Mt. Res. Dev., 29 (2009), pp. 350-355, 10.1659/mrd.00007
View Record in Scopus   Google Scholar

Chen et al., 2004   R. Chen, K. Ersi, J. Yang, S. Lu, W. Zhao
Validation of five global radiation models with measured daily data in China
Energy Convers. Manag., 45 (2004), pp. 1759-1769, 10.1016/j.enconman.2003.09.019
Article   📄 Download PDF   View Record in Scopus   Google Scholar

Córdova et al., 2015   M. Córdova, G. Carrillo-Rojas, P. Crespo, B. Wilcox, R. Célleri
Evaluation of the Penman-Monteith (FAO 56 PM) method for calculating reference evapotranspiration using limited data
Mt. Res. Dev. (2015), p. 230, 10.1659/mrd-journal-d-14-0024.1
View Record in Scopus   Google Scholar

Vanderlinden et al., 2004   K. Vanderlinden, J.V. Giráldez, M. Van Meirvenne
Assessing reference evapotranspiration by the hargreaves method in Southern Spain
J. Irrig. Drain. Eng., 130 (2004), pp. 184-191, 10.1061/(ASCE)0733-9437(2004)130:3(184)
View Record in Scopus   Google Scholar

Doorenbos and Pruitt, 1977 J. Doorenbos, W.O. Pruitt

Guidelines for predicting crop water requirements

FAO Irrig. Drain. Pap., 24 (1977), p. 144

Google Scholar

Feng et al., 2019 Y. Feng, D. Gong, Q. Zhang, S. Jiang, L. Zhao, N. Cui

Evaluation of temperature-based machine learning and empirical models for predicting daily global solar radiation

Energy Convers. Manag., 198 (2019), Article 111780, 10.1016/j.enconman.2019.111780

Article　　Download PDF　　View Record in Scopus　　Google Scholar

Garcia et al., 2004 M. Garcia, D. Raes, R. Allen, C. Herbas

Dynamics of reference evapotranspiration in the Bolivian highlands (Altiplano)

Agric. . Meteorol., 125 (2004), pp. 67-82, 10.1016/j.agrformet.2004.03.005

Article　　Download PDF　　View Record in Scopus　　Google Scholar

Garreaud, 2009 R.D. Garreaud

The Andes climate and weather

Adv. Geosci., 22 (2009), pp. 3-11, 10.5194/adgeo-22-3-2009

View Record in Scopus　　Google Scholar

Hargreaves and Samani, 1982 George H. Hargreaves, Zohrab A. Samani

Estimating potential evapotranspiration

J. Irrig. Drain. Div., 108 (1982), pp. 225-230

CrossRef　　View Record in Scopus　　Google Scholar

Hofstede et al., 2014 R. Hofstede, J. Calles, V. López, R. Polanco, F. Torres, J. Ulloa, A. Vásquez, M.C

LOS PÁRAMOS ANDINOS ¿Qué Sabemos? Estado de conocimiento sobre el impacto del cambio climático en el ecosistema páramo

UICN Quito Ecuad. (2014), pp. 7-61, 10.2307/j.ctvpv50bh.8

Google Scholar

Ishak et al., 2010 A.M. Ishak, M. Bray, R. Remesan, D. Han

Estimating reference evapotranspiration using numerical weather modelling

Hydrol. Process., 24 (2010), pp. 3490-3509, 10.1002/hyp.7770

View Record in Scopus　　Google Scholar

Jabloun and Sahli, 2008 M. Jabloun, A. Sahli

Evaluation of FAO-56 methodology for estimating reference evapotranspiration using limited climatic data

Appl. Tunis. Agric. Water Manag., 95 (2008), pp. 707-715, 10.1016/j.agwat.2008.01.009

Article　　Download PDF　　View Record in Scopus　　Google Scholar

Jeong et al., 2017 D.I. Jeong, A. St-Hilaire, Y. Gratton, C. Bélanger, C. Saad

A guideline to select an estimation model of daily global solar radiation between geostatistical interpolation and stochastic simulation approaches

Renew. Energy, 103 (2017), pp. 70-80, 10.1016/j.renene.2016.11.022

Article   📄 Download PDF   View Record in Scopus   Google Scholar

De Jong and Stewart, 1993   R. De Jong, D.W. Stewart

Estimating global solar radiation from common meteorological observations in western Canada

Can. J. Plant Sci., 73 (1993), pp. 509-518, 10.4141/cjps93-068

View Record in Scopus   Google Scholar

Karimi et al., 2020   S. Karimi, J. Shiri, P. Marti

Supplanting missing climatic inputs in classical and random forest models for estimating reference evapotranspiration in humid coastal areas of Iran

Comput. Electron. Agric., 176 (2020), Article 105633, 10.1016/j.compag.2020.105633

Article   📄 Download PDF   View Record in Scopus   Google Scholar

Kottek et al., 2006   M. Kottek, J. Grieser, C. Beck, B. Rudolf, F. Rubel

World map of the Köppen-Geiger climate classification updated

Meteorol. Z., 15 (2006), pp. 259-263, 10.1127/0941-2948/2006/0130

Google Scholar

Landeras et al., 2008   G. Landeras, A. Ortiz-Barredo, J.J. López

Comparison of artificial neural network models and empirical and semi-empirical equations for daily reference evapotranspiration estimation in the Basque Country (Northern Spain)

Agric. Water Manag., 95 (2008), pp. 553-565, 10.1016/j.agwat.2007.12.011

Article   📄 Download PDF   View Record in Scopus   Google Scholar

Liu et al., 2009   X. Liu, X. Mei, Y. Li, Q. Wang, J.R. Jensen, Y. Zhang, J.R. Porter

Evaluation of temperature-based global solar radiation models in China

Agric. . Meteorol., 149 (2009), pp. 1433-1446, 10.1016/j.agrformet.2009.03.012

Article   📄 Download PDF   View Record in Scopus   Google Scholar

Li et al., 2014   H. Li, F. Cao, X. Wang, W. Ma

A temperature-based model for estimating monthly average daily global solar radiation in China

Sci. World J., 2014 (2014), 10.1155/2014/128754

Google Scholar

Li et al., 2013   M.F. Li, L. Fan, H. Liu, Bin, P.T. Guo, W. Wu

A general model for estimation of daily global solar radiation using air temperatures and site geographic parameters in Southwest China

J. Atmos. Sol. Terr. Phys., 92 (2013), pp. 145-150, 10.1016/j.jastp.2012.11.001

Article   📄 Download PDF   View Record in Scopus   Google Scholar

Llambí et al., 2012   Llambí, L.D., Soto, A., Célleri, R., De Bievre, B., Ochoa, B., Borja, P., 2012. Ecología, Hidrología y Suelos de Páramos. Proy. Páramo Andin. 284.
Google Scholar

Ministerio de Agricultura y Ganadería et al., 2019   Ministerio de Agricultura y Ganadería, M., Instituto Interamericano de Cooperación para la Agricultura, I., Gobiernos Autónomos Descentralizados Provinciales, CONGOPE, C. de G.A.P. del E–, DHSA, D.H. de la S. del A., OG, O. de R., Foro de los Recursos Hídricos, F., 2019. Plan Nacional de Riego y Drenaje.
Google Scholar

Motavita et al., 2019   D.F. Motavita, R. Chow, A. Guthke, W. Nowak
The comprehensive differential split-sample test: a stress-test for hydrological model robustness under climate variability
J. Hydrol., 573 (2019), pp. 501-515, 10.1016/j.jhydrol.2019.03.054
Article   Download PDF   View Record in Scopus   Google Scholar

Ochoa-Sánchez et al., 2019   A. Ochoa-Sánchez, P. Crespo, G. Carrillo-Rojas, A. Sucozhañay, R. Célleri
Actual evapotranspiration in the high andean grasslands: a comparison of measurement and estimation methods
Front. Earth Sci., 7 (2019), pp. 1-16, 10.3389/feart.2019.00055
View Record in Scopus   Google Scholar

Paredes et al., 2017   P. Paredes, J.C. Fontes, E.B. Azevedo, L.S. Pereira
Daily reference crop evapotranspiration with reduced data sets in the humid environments of Azores islands using estimates of actual vapor pressure, solar radiation, and wind speed
Theor. Appl. Climatol., 134 (2017), pp. 1115-1133, 10.1007/s00704-017-2329-9
Google Scholar

Paredes and Pereira, 2019   P. Paredes, L.S. Pereira
Computing FAO56 reference grass evapotranspiration PM-ET o from temperature with focus on solar radiation
Agric. Water Manag., 215 (2019), pp. 86-102, 10.1016/j.agwat.2018.12.014
Article   Download PDF   View Record in Scopus   Google Scholar

Paredes et al., 2020   P. Paredes, L.S. Pereira, J. Almorox, H. Darouich
Reference grass evapotranspiration with reduced data sets: Parameterization of the FAO Penman-Monteith temperature approach and the Hargeaves-Samani equation using local climatic variables
Agric. Water Manag., 240 (2020), Article 106210, 10.1016/j.agwat.2020.106210
Article   Download PDF   View Record in Scopus   Google Scholar

Paredes et al., 2021   P. Paredes, I. Trigo, H. de Bruin, N. Simões, L.S. Pereira

Daily grass reference evapotranspiration with Meteosat second generation shortwave radiation and reference ET products

Agric. Water Manag. (2021), p. 248, 10.1016/j.agwat.2020.106543

    Google Scholar

Perrin et al., 2007   C. Perrin, L. Oudin, V. Andreassian, C. Rojas-Serna, C. Michel, T. Mathevet

Impact of limited streamflow data on the efficiency and the parameters of rainfall-runoff models

Hydrol. Sci. J., 52 (2007), pp. 131-151, 10.1623/hysj.52.1.131

    View Record in Scopus   Google Scholar

Qadeer et al., 2021   K. Qadeer, A. Ahmad, M.A. Qyyum, A.S. Nizami, M. Lee

Developing machine learning models for relative humidity prediction in air-based energy systems and environmental management applications

J. Environ. Manag., 292 (2021), Article 112736, 10.1016/j.jenvman.2021.112736

Article   Download PDF   View Record in Scopus   Google Scholar

Raziei and Pereira, 2013   T. Raziei, L.S. Pereira

Estimation of ETo with hargreaves-samani and FAO-PM temperature methods for a wide range of climates in Iran

Agric. Water Manag., 121 (2013), pp. 1-18, 10.1016/j.agwat.2012.12.019

Article   Download PDF   View Record in Scopus   Google Scholar

Ren et al., 2016   X. Ren, Z. Qu, D.S. Martins, P. Paredes, L.S. Pereira

Daily reference evapotranspiration for hyper-arid to moist sub-humid climates in inner Mongolia, China: I. Assessing temperature methods and spatial variability

Water Resour. Manag., 30 (2016), pp. 3769-3791, [10.1007/s11269-016-1384-9](10.1007/s11269-016-1384-9)

    View Record in Scopus   Google Scholar

Samani, 2000   Z. Samani

Self-calibrating method for estimating solar radiation from air temperature

J. Irrig. Drain. Eng., 126 (2000), pp. 265-267

    View Record in Scopus   Google Scholar

Santos et al., 2020   J.E.O. Santos, F.F. da Cunha, R. Filgueiras, G.H. da Silva, A.H. de Castro Teixeira, F.C. dos Santos Silva, G.C. Sediyama

Performance of Safer evapotranspiration using missing meteorological data

Agric. Water Manag., 233 (2020), Article 106076, 10.1016/j.agwat.2020.106076

Article   Download PDF   View Record in Scopus   Google Scholar

Sentelhas et al., 2010   P.C. Sentelhas, T.J. Gillespie, E.A. Santos

Evaluation of FAO Penman-Monteith and alternative methods for estimating reference evapotranspiration with missing data in Southern Ontario

Can. Agric. Water Manag., 97 (2010), pp. 635-644, 10.1016/j.agwat.2009.12.001

Article   Download PDF   View Record in Scopus   Google Scholar

da Silva et al., 2018   G.H. da Silva, S.H.B. Dias, L.B. Ferreira, J.É.O. Santos, F.F. da Cunha
Performance of different methods for reference evapotranspiration estimation in Jaíba, Brazil
Rev. Bras. Eng. Agric. E Ambient., 22 (2018), pp. 83-89, 10.1590/1807-1929/agriambi.v22n2p83-89
View Record in Scopus   Google Scholar

Silva et al., 2010   D. Silva, F.J. Meza, E. Varas
Estimating reference evapotranspiration (ETo) using numerical weather forecast data in central Chile
J. Hydrol., 382 (2010), pp. 64-71, 10.1016/j.jhydrol.2009.12.018
Article   Download PDF   View Record in Scopus   Google Scholar

Tabari et al., 2016   H. Tabari, P. Hosseinzadehtalaei, P. Willems, C. Martinez
Validation and calibration of solar radiation equations for estimating daily reference evapotranspiration at cool semi-arid and arid locations
Hydrol. Sci. J., 61 (2016), pp. 610-619, 10.1080/02626667.2014.947293
View Record in Scopus   Google Scholar

Todorovic et al., 2013   M. Todorovic, B. Karic, L.S. Pereira
Reference evapotranspiration estimate with limited weather data across a range of Mediterranean climates
J. Hydrol., 481 (2013), pp. 166-176, 10.1016/j.jhydrol.2012.12.034
Article   Download PDF   View Record in Scopus   Google Scholar

Tomas-Burguera et al., 2017   M. Tomas-Burguera, S.M. Vicente-Serrano, M. Grimalt, S. Beguería
Accuracy of reference evapotranspiration (ETo) estimates under data scarcity scenarios in the Iberian Peninsula
Agric. Water Manag., 182 (2017), pp. 103-116, 10.1016/j.agwat.2016.12.013
Article   Download PDF   View Record in Scopus   Google Scholar

UNEP, 1992   UNEP
United nations environment programme
World Atlas of Desertification (2nd. ed.,), Oxford University Press (1992)
Google Scholar

Wright et al., 2018   C. Wright, A. Kagawa-Viviani, C. Gerlein-Safdi, G.M. Mosquera, M. Poca, H. Tseng, K.P. Chun
Advancing ecohydrology in the changing tropics: perspectives from early career scientists
Ecohydrology, 11 (2018), 10.1002/eco.1918
Google Scholar

Xia et al., 2004   Y. Xia, Z.L. Yang, C. Jackson, P.L. Stoffa, M.K. Sen

Impacts of data length on optimal parameter and uncertainty estimation of a land surface model

J. Geophys. Res. D. Atmos. (2004), p. 109, [10.1029/2003jd004419](#)

Google Scholar

Cited by (2)

Influence of ENSO on Droughts and Vegetation in a High Mountain Equatorial Climate Basin

2022, Atmosphere

Daily Prediction and Multi-Step Forward Forecasting of Reference Evapotranspiration Using LSTM and Bi-LSTM Models

2022, Agronomy

View Abstract